

UNCLASSIFIED

DEFENCE RESEARCH ESTABLISHMENT
CENTRE DE RECHERCHES POUR LA DÉFENSE
VALCARTIER, QUÉBEC

DREV – TM – 9814

Unlimited Distribution / Distribution illimitée

**IMPULSE ON BLAST DEFLECTORS
FROM A LANDMINE EXPLOSION**

by

J.E. Tremblay

September / septembre 1998

Approved by / approuvé par

R. Delagrave

Head, Weapons Effects Section

Chef, Section effets des armes

SANS CLASSIFICATION

ABSTRACT

Anti-mine blast deflectors are now used as a standard countermeasure to reduce landmine effects on a vehicle's occupants, increasing their chances of survival. The blast deflectors are submitted to an impulse from the soil ejecta and detonation products resulting from a mine explosion. This memorandum presents algebraic equations to estimate the total impulse imparted to these deflectors. The proposed equations are suitable for use in a spreadsheet program and can be used by engineers and scientists to develop anti-mine protection systems.

RÉSUMÉ

Des déflecteurs de souffle antimine sont maintenant utilisés de façon standard pour diminuer les effets de mines sur les occupants d'un véhicule, augmentant ainsi leurs chances de survie. Les déflecteurs de souffle sont soumis à l'impulsion causée par le sol et aux produits de détonation résultant de l'explosion d'une mine. Ce mémorandum présente des équations algébriques pour estimer l'impulsion totale transmise à ces déflecteurs. Ces équations peuvent être programmées dans un chiffrier électronique et utilisées par les ingénieurs et scientifiques qui mettent au point les systèmes de protection antimine.

TABLE OF CONTENTS

ABSTRACT / RÉSUMÉ	i
EXECUTIVE SUMMARY	v
LIST OF FIGURES / TABLES	vii
1 INTRODUCTION	1
2 REFERENCE SYSTEM	2
3 FUNDAMENTAL MODEL	2
3.1 Vertical Component of the Specific Impulse	3
3.2 Modified Empirical Function	5
4 HORIZONTAL BLAST DEFLECTORS	7
4.1 Total Impulse	7
4.2 Approximate Solution	7
4.3 Square Deflectors Centered above the Mine	10
5 OBLIQUE BLAST DEFLECTORS	11
5.1 Specific Impulse	11
5.2 Total Impulse	13
5.3 Approximate Solution	14
5.4 Deflectors Centered on the x Axis	18
6 VERTICAL BLAST DEFLECTORS	19
6.1 Specific Impulse	19
6.2 Total Impulse	19
6.3 Approximate Solution	20
7 CONCLUSIONS	24
8 ACKNOWLEDGMENTS	24
9 REFERENCES	25
APPENDIX—The Error Function	26
FIGURES 1 to 18	
TABLES I to II	

EXECUTIVE SUMMARY

Landmines, also called anti-tank mines, vehicle mines or simply mines, have been encountered in recent peacekeeping missions in Cambodia, Somalia and Bosnia. Even though the Canadian Forces have acquired some mine-proof vehicles from South Africa, there is a need to develop anti-mine protection systems for the Canadian B-fleet, ranging from the light support vehicle wheeled (LSVW) to the heavy engineer support vehicle (HESV). To help meet this requirement, the Defence Research Establishment Valcartier has undertaken a defence R&D project to better protect the occupants of soft-skinned vehicles from landmine effects.

The capability of estimating the impulse transmitted to a vehicle is essential to predict or simulate the motion of the vehicle and its occupants subjected to a landmine explosion. This memorandum provides algebraic equations to estimate the total impulse on vehicle plates acting as blast deflectors—an important counter-measure to deflect mine effects away from the vehicle's occupants. These equations are applied in a series of examples to obtain an estimate of the magnitude of the expected impulses and to study the effects of some changes in the mine/target geometry on the resulting impulses.

The impulse produced from a landmine explosion is mainly the result of detonation products and soil ejecta impacting the target at high velocity. The U.S. Army Tank-Automotive & Armaments Command developed in 1985 an empirical equation to predict the vertical component of the specific impulse (impulse per unit area) for buried charges with a pancake shape. That vertical component of the specific impulse is used in this memorandum to derive algebraic equations for the total impulse on horizontal, oblique and vertical blast deflectors. An expression for the maximum impulse to be expected for a given standoff distance is also presented.

These equations will be used in the development of efficient anti-mine protection systems at DREV. However, more research is required to combine the impulse on blast deflectors to the impulse on a wheel for an explosion under a tire.

LIST OF FIGURES

1	The Coordinates System	3
2	Horizontal Blast Deflector	4
3	The Approximation of $f(\zeta d)$ by $g(\zeta d)$	6
4	The Absolute Error $f(\zeta d) - g(\zeta d)$	6
5	Horizontal Blast Deflector over the xy -Plane	7
6	Total Impulse as a Function of Plate Width for Ex. 2	11
7	Total Impulse as a Function of Standoff Distance for Ex. 3	12
8	Oblique Blast Deflector	12
9	Pressure Area for i_n and i_r	13
10	Oblique Blast Deflector over the xyz -Plane	14
11	V-Shaped Blast Deflector Centered Above the Mine	16
12	Graph of $\zeta(z(x))$ for Ex. 4	17
13	Graph of Eq. (36) with the Parameters of Ex. 4	17
14	Vertical Blast Deflector	20
15	Graph of Eq. (44) for Ex. 6	21
16	Total Impulse as a Function of x_0 for Ex. 6	21
17	V-Shaped deflector of Variable Angle γ	22
18	Impulse as a Function of the Angle γ in Fig. 17	23

LIST OF TABLES

I	Gauss-Legendre Abscissas and Weights	18
II	Impulse on the Variable V-Shaped Deflector for Ex. 7	23

1 INTRODUCTION

Since the last World War and the creation of the United Nations, Canada has been involved, to various degrees, in all UN peacekeeping missions. Landmines, also called anti-tank mines, vehicle mines or simply mines, have been encountered in recent peacekeeping missions in Cambodia, Somalia and Bosnia. While most UN missions do not put the lives of the peacekeepers at immediate stake, these three cited missions did indeed put soldiers in hazardous situations and good anti-mine protection systems should have been required for most of the vehicles.

In Bosnia, 53% of landmine accidents occurred while the vehicles hit mines on “cleared routes” (see [1]), showing that in a mine-infested region, one must always be protected from landmine effects. Even though the Canadian Forces have acquired some mine-proof vehicles from South Africa, there is a need to develop anti-mine protection systems for the Canadian B-fleet, ranging from the light support vehicle wheeled (LSVW) to the heavy engineer support vehicle (HESV). To help meet this requirement, the Defence Research Establishment Valcartier has undertaken a defence R&D project to better protect the occupants of soft-skinned vehicles from landmine effects (see [2, 3]).

To predict or simulate the motion of a vehicle and its occupants submitted to a landmine explosion, one needs the capability of predicting the impulse transmitted to the vehicle. This technical memorandum provides algebraic equations to estimate the total impulse on vehicle plates acting as blast deflectors—an important counter-measure to redirect the mine effects away from the vehicle’s occupants. These equations are applied in a series of seven examples to obtain an estimate of the magnitude of the expected impulses and to study the effects of various changes in the mine/target geometry on the resulting impulses.

These algebraic equations will be helpful to the engineers who need to estimate

the loads for the design of blast deflectors, and to the scientists who develop anti-mine protection systems.

To describe the mine/target geometry, a fixed system of coordinates (the observer's view) is first defined in Chapter 2.

Westin et al. in [4] have developed an empirical equation for the specific impulse transmitted to plates. Chapter 3 proposes an approximation of that empirical equation from which derived algebraic equations for the total impulse are found and presented in Chapter 4 for horizontal deflectors; in Chapter 5 for oblique deflectors; and in Chapter 6 for vertical deflectors.

This work was carried out at DREV under project work unit 2ba15, *Survivability and Lethality Assessment and Modeling Software*, between January and March 1998.

2 REFERENCE SYSTEM

The origin O of the \mathbf{xyz} -axes is located at the center of the mine, buried at a depth δ , as shown in Fig. 1. The horizontal plane is the \mathbf{xy} -plane and the \mathbf{z} -axis points towards the sky.

3 FUNDAMENTAL MODEL

The impulse produced from a landmine explosion is mainly the result of detonation products and soil ejecta impacting the target at high velocity (see [4]). The loading generated from the impulse is characterized by a high pressure during a short period of time. The duration is much shorter than the natural period of the vehicle

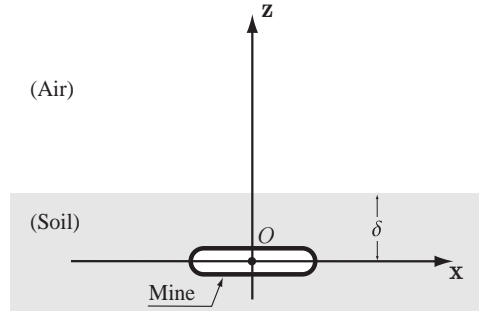


FIGURE 1 – The Coordinates System

structure, and so the exact shape of the pressure-time loading is not as important for the calculation of the vehicle's response as its integral over time. The integral of the pressure loading over time is called the specific impulse.

In [4], Westin et al. proposed an empirical equation to predict the vertical component of the specific impulse (impulse per unit area) for buried charges with a pancake shape. The vertical component of the specific impulse is fundamental for the characterization of the total impulse since, as will be shown in Chapters 5 and 6, the other components are easily derived from the vertical component.

3.1 Vertical Component of the Specific Impulse

Let $P = P(x, y, z)$ be a point on a horizontal blast deflector, as shown in Fig. 2. The empirical expression for the vertical specific impulse i_v at P is, from [4],

$$i_v(x, y) = 0.1352 \left(1 + \frac{7\delta}{9z} \right) \left(\frac{\tanh(0.9589\zeta d)}{\zeta d} \right)^{3.25} \sqrt{\frac{\rho E}{z}} \quad [\text{Pa}\cdot\text{s}] \quad (1)$$

where

z = standoff distance of P to the center of the mine [m]

$d = \sqrt{x^2 + y^2}$ = lateral distance to center of the mine [m]

δ = burial depth to center of the mine [m]

ρ = soil density [kg/m³]

E = energy release in explosive charge [J]

\mathcal{A} = cross-sectional area of the mine [m²]

and

$$\zeta = \frac{\delta}{z^{5/4} \mathcal{A}^{3/8} \tanh\left(\left(2.2 \frac{\delta}{z}\right)^{3/2}\right)} \quad [\text{m}^{-1}] \quad .$$

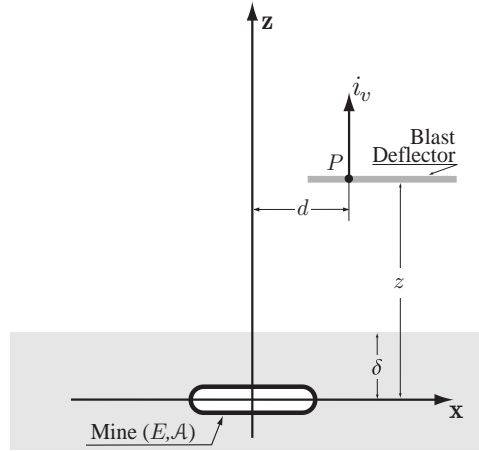


FIGURE 2 – Horizontal Blast Deflector

Because Eq. (1) is an empirical one, it should be used only when those four criteria are all met:

$$0.106 \leq \frac{\delta}{z} \leq 1.00 \quad (2)$$

$$6.35 \leq \frac{E/\mathcal{A}}{\rho c^2 z} \leq 150.0 \quad (3)$$

$$0.154 \leq \frac{\sqrt{\mathcal{A}}}{z} \leq 4.48 \quad (4)$$

$$0 \leq \frac{d}{z} \leq 19.3 \quad (5)$$

The parameter c in Eq. (3) is the seismic P-wave velocity in the soil expressed in [m/s].

The function

$$f(\zeta d) \stackrel{\text{def}}{=} \left(\frac{\tanh(0.9589 \zeta d)}{\zeta d} \right)^{3.25} \quad (6)$$

in Eq. (1) is not defined at $\zeta d = 0$; when $\zeta d \rightarrow 0$, $f(\zeta d)$ goes to

$$\lim_{\zeta d \rightarrow 0} f(\zeta d) = (0.9589)^{3.25} = 0.8725.$$

Then for small values of ζd (*e.g.* $\zeta d < 0.05$) Eq. (1) for the vertical component of the impulse becomes

$$i_v(x, y) \simeq 0.1180 \left(1 + \frac{7\delta}{9z} \right) \sqrt{\frac{\rho E}{z}}. \quad (7)$$

3.2 Modified Empirical Function

The total impulse on a blast deflector is given by the integral of the specific impulse over the total area of that blast deflector.

$$i_v = \iint_{\mathbb{A}} i_v(x, y) dx dy \quad [\text{N}\cdot\text{s}].$$

An algebraic equation for the total impulse is sought in this memorandum. To integrate analytically Eq. (1) is made impossible by the form of the function $f(\zeta d)$ defined with Eq. (6). The solution proposed in this document is to approximate $f(\zeta d)$

by a function for which an analytical solution of the integral of the specific impulse over the entire plate surface exists. The function $g(\zeta d)$ defined as

$$f(\zeta d) \approx g(\zeta d) \stackrel{\text{def}}{=} \kappa_1 \left(1 + \kappa_2 (\zeta d)^6\right) e^{-\kappa_3 (\zeta d)^2}, \quad g(0) = \lim_{\zeta d \rightarrow 0} f(\zeta d) \quad (8)$$

meets this requirement and its parameters were sought using the *Mathematica*TM function `NonlinearFit` (see [5]). The best values for the fit are

$$\kappa_1 = 0.8725, \quad \kappa_2 = 0.04837, \quad \kappa_3 = 0.8917. \quad (9)$$

Fig. 3 compares the functions f and g and the absolute error $f - g$ is plotted in Fig. 4.

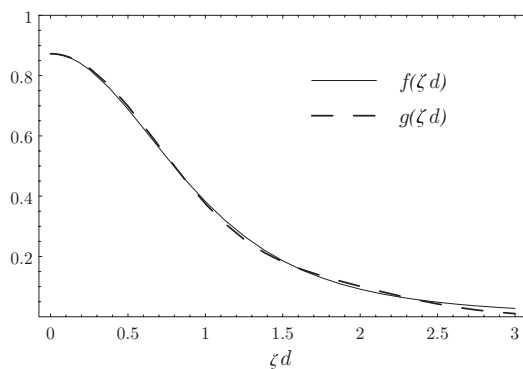


FIGURE 3 – The Approximation of $f(\zeta d)$ by $g(\zeta d)$

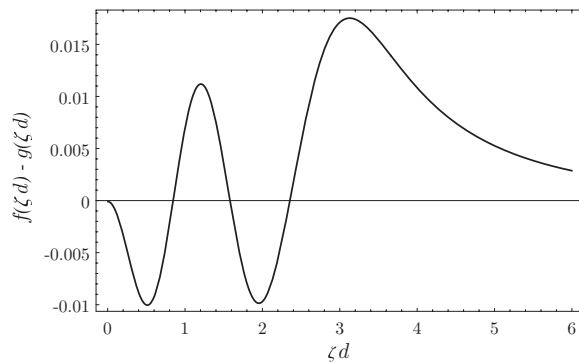


FIGURE 4 – The Absolute Error $f(\zeta d) - g(\zeta d)$

4 HORIZONTAL BLAST DEFLECTORS

4.1 Total Impulse

The total impulse i_v on a horizontal blast deflector is given by the integral of the specific impulse $i_v(x, y)$ over the entire plate surface. If the projection of the blast deflector on the \mathbf{xy} -plane is as seen in Fig. 5, then the total vertical impulse on the deflector is

$$\begin{aligned} i_v &= \int_{x_0}^{x_1} \int_{y_0}^{y_1} i_v(x, y) dy dx \\ &= 0.1352 \left(1 + \frac{7\delta}{9z}\right) \sqrt{\frac{\rho E}{z}} \int_{x_0}^{x_1} \int_{y_0}^{y_1} f(\zeta d) dy dx . \end{aligned} \quad (10)$$

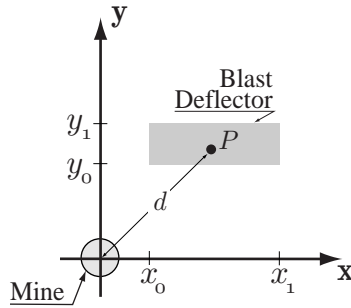


FIGURE 5 – Horizontal Blast Deflector over the \mathbf{xy} -Plane

4.2 Approximate Solution

There are no known analytical solution for the integral in Eq. (10). This integral can be numerically integrated but the process is time consuming and does not generate an algebraic equation for the total impulse. The solution proposed is to use the approximation (8) to replace $f(\zeta d)$ by $g(\zeta d)$ in Eq. (10).

The vertical impulse on the deflector can now be rewritten as

$$\boxed{i_v = \kappa_0 (S_1 + S_2) \left(1 + \frac{7\delta}{9z}\right) \sqrt{\frac{\rho E}{z}}} \quad (11)$$

where

$$\kappa_0 = 0.1352 \kappa_1 = 0.1180 \quad (12)$$

$$S_1 = \int_{x_0}^{x_1} \int_{y_0}^{y_1} e^{-\kappa_3(\zeta d)^2} dy dx = \frac{\pi \Delta_x \Delta_y}{4 \kappa_3 \zeta^2} \quad (13)$$

$$S_2 = \int_{x_0}^{x_1} \int_{y_0}^{y_1} \kappa_2 (\zeta d)^6 e^{-\kappa_3(\zeta d)^2} dy dx = \frac{\kappa_2}{16 \kappa_3^4 \zeta^2} \sum_{i=1}^5 A_i \quad (14)$$

$$\Delta_x = \operatorname{erf}(\sqrt{\kappa_3} x_1 \zeta) - \operatorname{erf}(\sqrt{\kappa_3} x_0 \zeta) \quad (15)$$

$$\Delta_y = \operatorname{erf}(\sqrt{\kappa_3} y_1 \zeta) - \operatorname{erf}(\sqrt{\kappa_3} y_0 \zeta) \quad (16)$$

$$\begin{aligned} A_1 = & \sqrt{\kappa_3} x_1 \zeta e^{-\kappa_3 x_1^2 \zeta^2} \times \\ & \left[12 \sqrt{\kappa_3} \zeta \left(e^{-\kappa_3 y_1^2 \zeta^2} \left(3 y_1 + \kappa_3 x_1^2 y_1 \zeta^2 + \kappa_3 y_1^3 \zeta^2 \right) \right. \right. \\ & \left. \left. - e^{-\kappa_3 y_0^2 \zeta^2} \left(3 y_0 + \kappa_3 x_1^2 y_0 \zeta^2 + \kappa_3 y_0^3 \zeta^2 \right) \right) \right. \\ & \left. - \sqrt{\pi} \Delta_y \left(33 + 16 \kappa_3 x_1^2 \zeta^2 + 4 \kappa_3^2 x_1^4 \zeta^4 \right) \right] \quad (17) \end{aligned}$$

$$\begin{aligned} A_2 = & 3 \sqrt{\kappa_3} x_0 \zeta e^{-\kappa_3 x_0^2 \zeta^2} \times \\ & \left[4 \zeta \sqrt{\kappa_3} \left(3 y_0 e^{-\kappa_3 y_0^2 \zeta^2} - 3 y_1 e^{-\kappa_3 y_1^2 \zeta^2} + \kappa_3 y_0^3 \zeta^2 e^{-\kappa_3 y_0^2 \zeta^2} \right. \right. \\ & \left. \left. - \kappa_3 y_1^3 \zeta^2 e^{-\kappa_3 y_1^2 \zeta^2} \right) + 11 \sqrt{\pi} \Delta_y \right] \quad (18) \end{aligned}$$

$$A_3 = -4 \sqrt{\pi} \kappa_3^{\frac{5}{2}} x_0^5 \zeta^5 \Delta_y e^{-\kappa_3 x_0^2 \zeta^2} \quad (19)$$

$$A_4 = 4 \kappa_3^{\frac{3}{2}} x_0^3 \zeta^3 e^{-\kappa_3 x_0^2 \zeta^2} \left[3 \zeta \sqrt{\kappa_3} \left(y_0 e^{-\kappa_3 y_0^2 \zeta^2} - y_1 e^{-\kappa_3 y_1^2 \zeta^2} \right) + 4 \sqrt{\pi} \Delta_y \right] \quad (20)$$

$$A_5 = \sqrt{\pi} \Delta_x \left[\frac{33 \sqrt{\kappa_3} y_0 \zeta}{e^{\kappa_3 y_0^2 \zeta^2}} - \frac{33 \sqrt{\kappa_3} y_1 \zeta}{e^{\kappa_3 y_1^2 \zeta^2}} + \frac{16 \kappa_3^{\frac{3}{2}} y_0^3 \zeta^3}{e^{\kappa_3 y_0^2 \zeta^2}} \right. \\ \left. - \frac{16 \kappa_3^{\frac{3}{2}} y_1^3 \zeta^3}{e^{\kappa_3 y_1^2 \zeta^2}} + \frac{4 \kappa_3^{\frac{5}{2}} y_0^5 \zeta^5}{e^{\kappa_3 y_0^2 \zeta^2}} - \frac{4 \kappa_3^{\frac{5}{2}} y_1^5 \zeta^5}{e^{\kappa_3 y_1^2 \zeta^2}} + 24 \sqrt{\pi} \Delta_y \right] \quad (21)$$

The function $\text{erf}(\cdot)$ in Eqs (15) and (16) is called the error function. The appendix gives the definition of the error function and presents an algorithm for its evaluation.

Example 1 To compare a numerical solution of Eq. (10) to the proposed algebraic solution (11), consider the explosion of a TMA-3 anti-tank mine under a vehicle equipped with a horizontal blast deflector installed 40 cm above the ground. The deflector area is 1 m by 1 m and is centered above the mine. The TMA-3 mine is 26.5 cm in diameter and 8 cm in height, contains 6.5 kg of cast TNT and is buried under 3 cm of soil of density 1.6 g/cm³. Then

$$z = 0.40 + 0.03 + \frac{0.08}{2} = 0.47 \quad [\text{m}] \\ x_0 = y_0 = -\frac{1}{2} \quad [\text{m}] \\ x_1 = y_1 = \frac{1}{2} \quad [\text{m}] \\ \delta = 0.03 + \frac{0.08}{2} = 0.07 \quad [\text{m}] \\ \rho = 1600 \quad [\text{kg/m}^3] \\ E = 6.5 \text{ [kg]} \times 4.516 \text{ [MJ/kg]} = 2.935 \cdot 10^7 \quad [\text{J}] \\ \mathcal{A} = \frac{\pi \times 0.265^2}{4} = 0.055 \quad [\text{m}^2] \\ \zeta = \frac{0.07}{(0.47)^{5/4} (0.055)^{3/8} \tanh\left(\left(2.2 \frac{0.07}{0.47}\right)^{3/2}\right)} = 2.879 \quad [\text{m}^{-1}]$$

Eq. (10) becomes

$$i_v = 0.1352 \left(1 + \frac{7(0.07)}{9(0.47)}\right) \sqrt{\frac{(1600)(2.935 \cdot 10^7)}{0.47}} \\ \times \iint \left(\frac{\tanh((0.9589)(2.897) d)}{2.897 d}\right)^{3.25} dx dy \\ = 1503 \times 4 \int_0^{1/2} \int_0^{1/2} \left(\frac{\tanh\left(2.778 \sqrt{x^2 + y^2}\right)}{\sqrt{x^2 + y^2}}\right)^{3.25} dx dy .$$

This integral was solved with the *Mathematica*TM function `NIntegrate`¹ resulting in $i_v \simeq 17.37$ [kN·s]. The evaluation of the algebraic Eq. (11) gives $i_v \simeq 17.38$ [kN·s], a difference of less than 0.07%.

¹The function `NIntegrate` is documented in [6]. It uses the Genz-Malik adaptive algorithm to solve the multidimensional integrals.

4.3 Square Deflectors Centered above the Mine

Consider a square blast deflector of width l centered above the mine. By substituting $x_1 = y_1 = l/2$ and $x_0 = y_0 = -l/2$ into Eqs (13) and (14), one gets

$$S_1 = \frac{\pi}{\kappa_3 \zeta^2} \operatorname{erf}^2(\sqrt{\kappa_3} l \zeta / 2) \quad (22)$$

and

$$S_2 = \frac{\kappa_2}{16 \kappa_3^4 \zeta^2} \left[(36 \kappa_3 l^2 \zeta^2 + 6 \kappa_3^2 l^4 \zeta^4) e^{-\kappa_3 l^2 \zeta^2 / 2} + 96 \pi \operatorname{erf}^2(\sqrt{\kappa_3} l \zeta / 2) - l \zeta \sqrt{\kappa_3} \pi (132 + 16 \kappa_3 l^2 \zeta^2 + \kappa_3^2 l^4 \zeta^4) \operatorname{erf}(\sqrt{\kappa_3} l \zeta / 2) e^{-\kappa_3 l^2 \zeta^2 / 4} \right]. \quad (23)$$

4.3.1 Effect of the Plate Area

When the area $\mathbb{A} = l^2$ of the blast deflector increases, the total vertical impulse increases also. However, if the standoff distance is kept constant, the impulse will eventually reach a limit value given by

$$\begin{aligned} \lim_{l \rightarrow \infty} i_v &= \kappa_0 \left(1 + \frac{7 \delta}{9 z} \right) \sqrt{\frac{\rho E}{z}} \lim_{l \rightarrow \infty} (S_1 + S_2) \\ &= \kappa_0 \left(1 + \frac{7 \delta}{9 z} \right) \sqrt{\frac{\rho E}{z}} \lim_{l \rightarrow \infty} \left[\frac{\pi}{\kappa_3 \zeta^2} \left(1 + \frac{6 \kappa_2}{\kappa_3^3} \right) \operatorname{erf}^2(\sqrt{\kappa_3} l \zeta / 2) \right] \\ &= \left(\frac{\kappa_0 \pi}{\kappa_3 \zeta^2} \right) \left(1 + \frac{6 \kappa_2}{\kappa_3^3} \right) \left(1 + \frac{7 \delta}{9 z} \right) \sqrt{\frac{\rho E}{z}}. \end{aligned}$$

Because the explosion of a mine under a deflector of infinite area is the worst possible case, this equation gives the upper limit of the impulse on any blast deflector

with a standoff distance of z meters:

$$\boxed{i_{\max} = \left(\frac{0.5857}{\zeta^2} \right) \left(1 + \frac{7\delta}{9z} \right) \sqrt{\frac{\rho E}{z}}} \quad (24)$$

Example 2 Consider the parameters of Ex. 1 on page 9 with, this time, a deflector l m wide by l m long. Fig. 6 is a plot of Eq. (11) with S_1 and S_2 given by (22) and (23), respectively. The maximum impulse computed with Eq. (24) is 24.9 [kN·s].

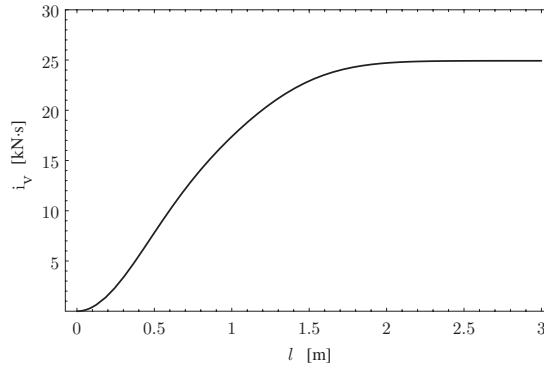


FIGURE 6 – Total Impulse as a Function of Plate Width for Ex. 2

4.3.2 Effect of the Standoff Distance

The total vertical impulse i_v decreases rapidly with the standoff distance z .

Example 3 Once again, consider the parameters of Ex. 1 on page 9. This time, the standoff distance goes from 15 cm to 4 m. Fig. 7 shows the decrease of the total impulse computed with Eq. (11).

5 OBLIQUE BLAST DEFLECTORS

5.1 Specific Impulse

When the blast deflector is not horizontal but at angle $0 < \alpha < \pi$ from the vertical, as in Fig. 8, the resulting specific impulse on the plate at location $P(x, y, z)$

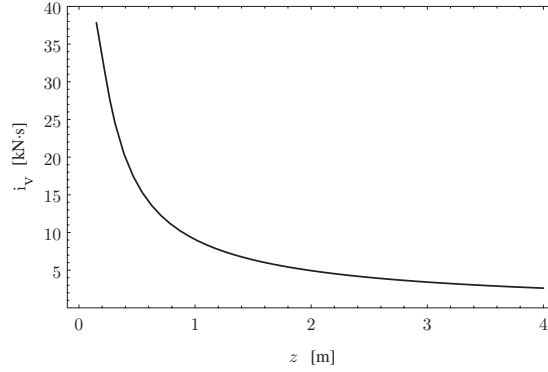


FIGURE 7 – Total Impulse as a Function of Standoff Distance for Ex. 3

is also a function of α .

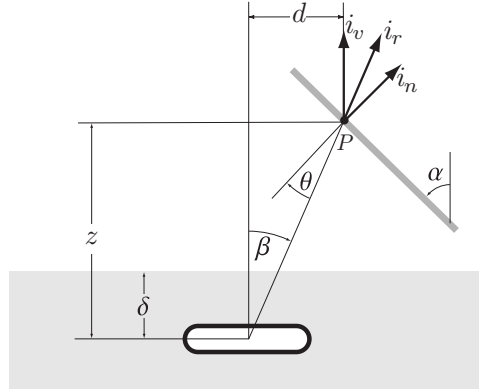


FIGURE 8 – Oblique Blast Deflector

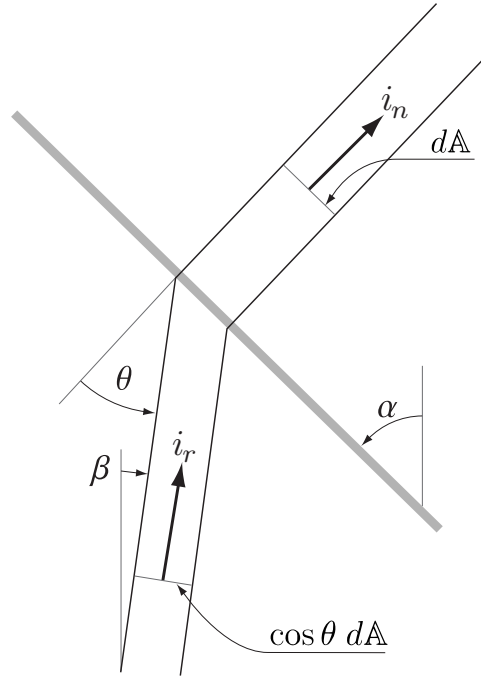
Let i_r be the radial specific impulse along the direction of the target point. From Fig. 9, the specific impulse i_n normal to the blast deflector is found from i_r by

$$(i_n)(d\Delta) = (i_r \cos \theta)(\cos \theta d\Delta)$$

or $i_n = i_r \cos^2 \theta$. Similarly, $i_v = i_r \cos^2 \beta$. By combining these last two equations together, one gets the relation between the known component of the specific impulse i_v to the sought component i_n ;

$$i_n = i_v \frac{\cos^2 \theta}{\cos^2 \beta} \quad . \quad (25)$$

Eq. (25) is different from the one used in [7], where the squares of the cosines are missing.

FIGURE 9 – Pressure Area for i_n and i_r

5.2 Total Impulse

For a blast deflector positioned as in Fig. 10, the deflector is in the plane $z = z_1 + (x_1 - x) \cot \alpha$. The area on which the impulse is applied is

$$\mathbb{A} = \frac{(x_1 - x_0)(y_1 - y_0)}{\sin \alpha} \quad (\text{oblique deflector surface})$$

and the element of integration $d\mathbb{A}$ is

$$d\mathbb{A} = \frac{dx dy}{\sin \alpha} .$$

The total normal impulse on the deflector is then

$$i_n = 0.1352 \int_{x_0}^{x_1} \int_{y_0}^{y_1} \left[\frac{\cos^2 \theta}{\cos^2 \beta \sin \alpha} \left(1 + \frac{7\delta}{9z} \right) f(\zeta d) \sqrt{\frac{\rho E}{z}} \right] dy dx \quad (26)$$

where

$$z = \lambda - x \cot \alpha \quad (27)$$

$$\lambda = z_1 + x_1 \cot \alpha \quad (28)$$

$$\cos \theta = \frac{x \cos \alpha + z \sin \alpha}{\sqrt{x^2 + y^2 + z^2}} \quad (29)$$

$$\cos \beta = \frac{z}{\sqrt{x^2 + y^2 + z^2}} . \quad (30)$$

The constant λ is the standoff distance when $x = 0$. By combining Eqs (27) to (30), the ratio of trigonometric functions in (26) becomes

$$\frac{\cos^2 \theta}{\cos^2 \beta \sin \alpha} = \frac{(x \cos \alpha + z \sin \alpha)^2}{z^2 \sin \alpha} = \frac{\lambda^2 \sin \alpha}{(\lambda - x \cot \alpha)^2} . \quad (31)$$

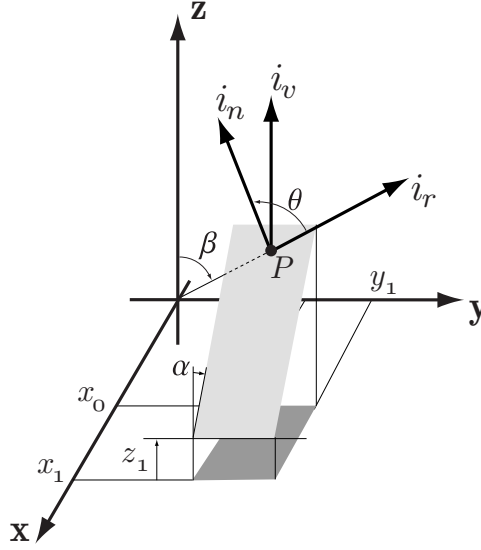


FIGURE 10 – Oblique Blast Deflector over the **xyz**-Plane

5.3 Approximate Solution

The total normal impulse i_n , as given by Eq. (26), cannot be analytically integrated. However, with the approximation (8), an algebraic solution can be obtained along the **y** axis. There is still a need to numerically integrate the resulting equation

along the \mathbf{x} axis but the number of summations drops at least from N^2 to N . For example, if a grid of 100 elements (as in [7]) are used to numerically integrate (26), four elements are usually enough with this proposed approximate solution (see Ex. 5–7).

5.3.1 Integration Along the y Axis

Substituting Eq. (8) into (26) and integrating along \mathbf{y} gives:

$$\begin{aligned} i_n &\simeq 0.1352 \int_{x_0}^{x_1} \int_{y_0}^{y_1} \frac{\cos^2 \theta}{\cos^2 \beta \sin \alpha} \left(1 + \frac{7\delta}{9z}\right) g(\zeta d) \sqrt{\frac{\rho E}{z}} dy dx \\ &= \kappa_0 \int_{x_0}^{x_1} \frac{\cos^2 \theta}{\cos^2 \beta \sin \alpha} \left(1 + \frac{7\delta}{9z}\right) \left[\Gamma_1(x, z) + \Gamma_2(x, z)\right] \sqrt{\frac{\rho E}{z}} dx \end{aligned} \quad (32)$$

where

$$\Gamma_1(x, z) = \frac{\Delta_y \sqrt{\pi}}{2 \zeta \sqrt{\kappa_3}} e^{-\kappa_3 \zeta^2 x^2} \quad (33)$$

$$\Gamma_2(x, z) = \frac{\kappa_2 e^{-\kappa_3 \zeta^2 x^2}}{16 \zeta \kappa_3^{7/2}} \left(\Lambda_2(x, z) + \sum_{i=0}^1 (-1)^{i+1} \Lambda_i(x, z) e^{-\kappa_3 \zeta^2 y_i^2} \right) \quad (34)$$

$$\zeta = \zeta(z) = \zeta(\lambda - x \cot \alpha)$$

$$\Lambda_2(x, z) = \Delta_y \sqrt{\pi} \left(15 + 18 \kappa_3 \zeta^2 x^2 + 12 \kappa_3^2 \zeta^4 x^4 + 8 \kappa_3^3 \zeta^6 x^6 \right)$$

$$\Lambda_i(x, z) = C_{i1} + C_{i2} (5 + 6 \kappa_3 \zeta^2 x^2) + C_{i3} (5 + 6 \kappa_3 \zeta^2 x^2 + 4 \kappa_3^2 \zeta^4 x^4)$$

$$C_{i1} = -8 \kappa_3^{5/2} \zeta^5 y_i^5 \quad C_{i2} = -4 \kappa_3^{3/2} \zeta^3 y_i^3$$

$$C_{i3} = -6 \kappa_3^{1/2} \zeta y_i \quad i = 0, 1$$

Eq. (32) can be rewritten as

$$i_n = \kappa_0 \int_{x_0}^{x_1} p(x) dx \quad (35)$$

where

$$\begin{aligned} p(x) &\stackrel{\text{def}}{=} \frac{\lambda^2 \sin \alpha}{(\lambda - x \cot \alpha)^2} \left(1 + \frac{7\delta}{9(\lambda - x \cot \alpha)}\right) \times \\ &\quad \left[\Gamma_1(x, z(x)) + \Gamma_2(x, z(x))\right] \sqrt{\frac{\rho E}{\lambda - x \cot \alpha}} \quad (36) \end{aligned}$$

Example 4 Consider a blast deflector made of two plates of size 0.5 m by 1 m each and attached in a V-shape, as shown in Fig. 11. The charge is a TMA-3 anti-tank mine buried with 3 cm of soil. The total impulse on the deflector is equivalent to four times the total impulse on the area contained in the region $x \in [0, 0.4]$ and $y \in [0, 0.5]$. Then, from Eq. (35)

$$i_n = 4 \kappa_0 \int_0^{0.4} p(x) dx$$

and from Fig. 11, $y_0 = 0$, $y_1 = 0.5$, $\cot \alpha = -0.75$ (or $\alpha = 126.9$ deg) and $z = 0.47 + 0.75x$. From Ex. 1 on page 9,

$$\begin{aligned} \delta &= 0.07 \quad [\text{m}] \\ \rho &= 1600 \quad [\text{kg/m}^3] \\ E &= 2.935 \cdot 10^7 \quad [\text{J}] \\ \mathcal{A} &= 0.055 \quad [\text{m}^2] \end{aligned}$$

and

$$\zeta = \frac{0.2077}{(0.47 + 0.75x)^{5/4} \tanh \left[0.0604 \left(\frac{1}{0.47 + 0.75x} \right)^{3/2} \right]} \quad [\text{m}^{-1}].$$

The function $\zeta = \zeta(z(x))$ for $0 \leq x \leq 0.4$ is plotted in Fig. 12 and is well approximated by the line

$$\zeta \simeq 2.887 + 0.872x.$$

The graph of $p(x)$ is shown in Fig. 13.

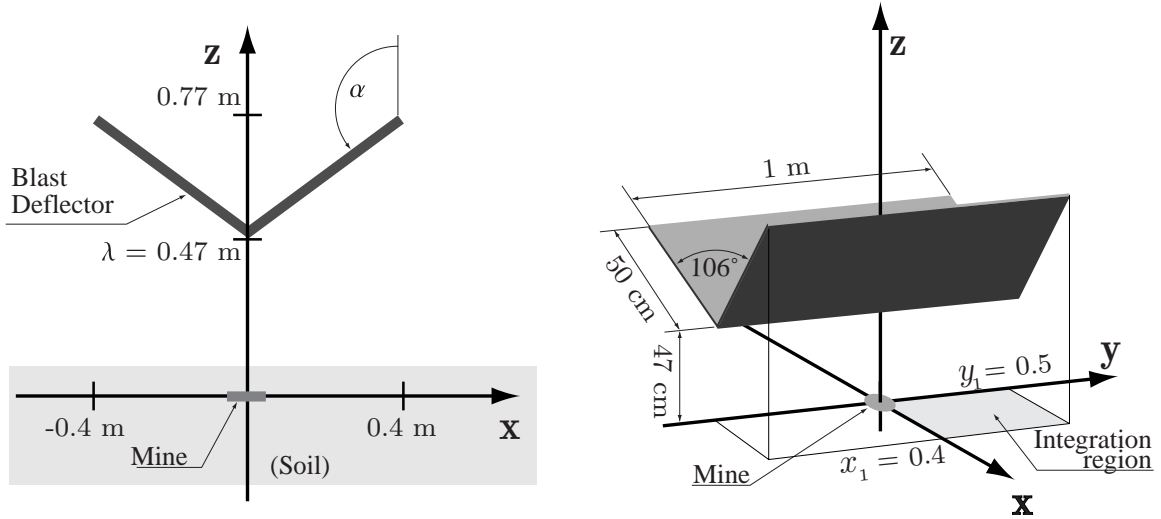


FIGURE 11 – V-Shaped Blast Deflector Centered Above the Mine

5.3.2 Integration Along the x Axis

Let

$$\xi = \frac{2x - x_0 - x_1}{x_1 - x_0};$$

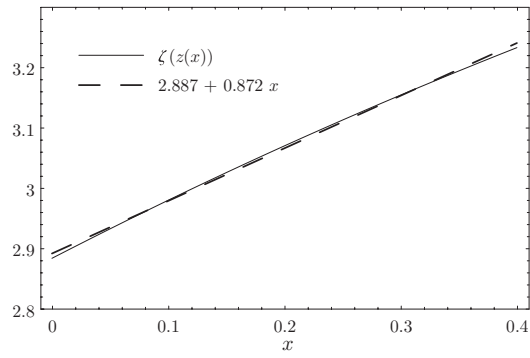
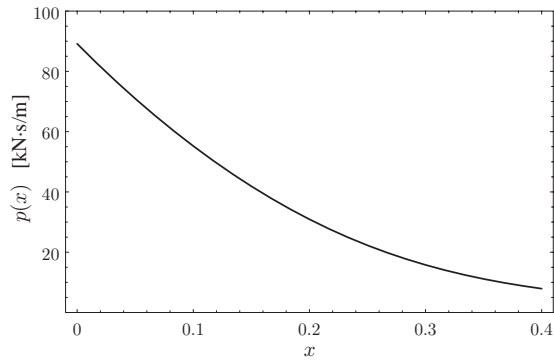
FIGURE 12 – Graph of $\zeta(z(x))$ for Ex. 4

FIGURE 13 – Graph of Eq. (36) with the Parameters of Ex. 4

then Eq. (35) becomes

$$\dot{i}_n = \kappa_0 \frac{x_1 - x_0}{2} \int_{-1}^1 p\left(\frac{\xi(x_1-x_0)+x_0+x_1}{2}\right) d\xi . \quad (37)$$

This equation can be numerically integrated using a Gaussian quadrature. A 4-point Gauss-Legendre integration is usually enough to integrate a smooth function such as $p(x)$ in Ex. 4 on page 16 (Fig. 13).

The total normal impulse on an oblique blast deflector can then be approximated by

$$\dot{i}_n \approx \kappa_0 \frac{x_1 - x_0}{2} \sum_{i=1}^N w_i p\left(\frac{\xi_i(x_1-x_0)+x_0+x_1}{2}\right) \quad (38)$$

where ξ_i and w_i are, respectively, the abscissas and weights of the N -point Gauss-Legendre quadrature formula. Values from [8] of ξ_i and w_i for $N = 4$ and 6 are shown in Table I.

TABLE I
Gauss-Legendre Abscissas and Weights

N	i	ξ_i	w_i
4	1, 2	$\pm 0.33998 \ 10435 \ 84856$	0.65214 51548 62546
	3, 4	$\pm 0.86113 \ 63115 \ 94053$	0.34785 48451 37454
6	1, 2	$\pm 0.23861 \ 91860 \ 83197$	0.46791 39345 72691
	3, 4	$\pm 0.66120 \ 93864 \ 66265$	0.36076 15730 48139
	5, 6	$\pm 0.93246 \ 95142 \ 03152$	0.17132 44923 79170

Example 5 The total impulse on the V-shaped deflector of Ex. 4 on page 16 is given by Eq. (38) as

$$\begin{aligned} \dot{i}_n &\simeq 4 \times 0.0236 [w_1 (p(0.1320) + p(0.2680)) + w_3 (p(0.0280) + p(0.3722))] \\ &= 6.97 \quad [\text{kN}\cdot\text{s}] . \end{aligned}$$

The integral (26) was solved with the *Mathematica*TM function `NIntegrate` resulting in $\dot{i}_n \simeq 6.99$ [kN·s], a difference of 0.3%.

5.4 Deflectors Centered on the x Axis

Let l be the length of the deflector along \mathbf{y} . Because the deflector is centered on the \mathbf{x} axis, the integral along \mathbf{y} for $-l/2 \leq y \leq l/2$ is twice the value of the integral

on the interval $0 \leq y \leq l/2$. Then Eqs (33) and (34), used in the calculation of $p(x)$, can be written as

$$\Gamma_1(x, z) = \operatorname{erf}(\sqrt{\kappa_3} \zeta l/2) \sqrt{\frac{\pi}{\kappa_3 \zeta^2}} e^{-\kappa_3 \zeta^2 x^2} \quad (39)$$

and

$$\Gamma_2(x, z) = \frac{\kappa_2 e^{-\kappa_3 \zeta^2 x^2}}{8 \kappa_3^{7/2} \zeta} \left\{ \left[-\kappa_3^{5/2} \zeta^5 l^5/4 - \kappa_3^{3/2} \zeta^3 l^3 (5 + 6 \kappa_3 \zeta^2 x^2)/2 - 3 \kappa_3^{1/2} \zeta l (5 + 6 \kappa_3 \zeta^2 x^2 + 4 \kappa_3^2 \zeta^4 x^4) \right] e^{-\kappa_3 \zeta^2 l^2/4} + \sqrt{\pi} (15 + 18 \kappa_3 \zeta^2 x^2 + 12 \kappa_3^2 \zeta^4 x^4 + 8 \kappa_3^3 \zeta^6 x^6) \operatorname{erf}(\sqrt{\kappa_3} \zeta l/2) \right\}. \quad (40)$$

6 VERTICAL BLAST DEFLECTORS

6.1 Specific Impulse

When the blast deflector is vertical, $\alpha = 0$ or π and the deflector is in the plane $x = x_0$ (Fig. 14). The deflector is in the region $y \in [y_0, y_1]$, $z \in [z_0, z_1]$ and an approach similar to Chapter 5 is applied. The ratio of cosines in Eq. (25) becomes

$$\frac{\cos^2 \theta}{\cos^2 \beta} = \left(\frac{x_0}{z} \right)^2$$

and the horizontal specific impulse on the vertical blast deflector is

$$i_h = i_v \left(\frac{x_0}{z} \right)^2. \quad (41)$$

6.2 Total Impulse

The total impulse on a vertical blast deflector is given by

$$i_h = 0.1352 \int_{z_0}^{z_1} \int_{y_0}^{y_1} \left[\left(\frac{x_0}{z} \right)^2 \left(1 + \frac{7 \delta}{9 z} \right) f(\zeta d) \sqrt{\frac{\rho E}{z}} \right] dy dz \quad (42)$$

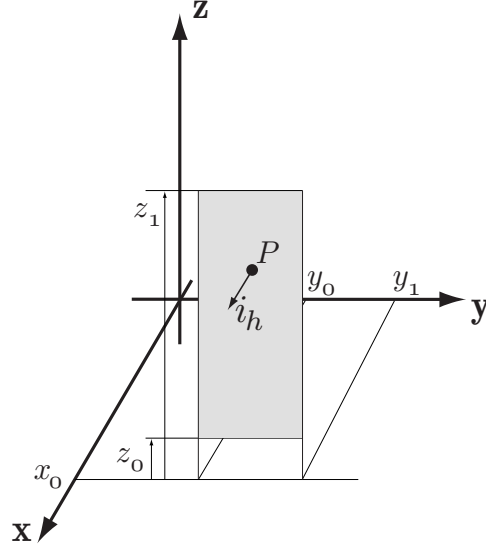


FIGURE 14 – Vertical Blast Deflector

where $d = \sqrt{x_0^2 + y^2}$.

6.3 Approximate Solution

By applying the method of Section 5.3, the total impulse on a vertical blast deflector can be written as

$$\dot{i}_h = \kappa_0 \int_{z_0}^{z_1} q(z) dz \quad (43)$$

where

$$q(z) \stackrel{\text{def}}{=} \frac{x_0^2 \sqrt{\rho E}}{z^{5/2}} \left(1 + \frac{7\delta}{9z} \right) \left[\Gamma_1(x_0, z) + \Gamma_2(x_0, z) \right] \quad (44)$$

and $\Gamma_1(x_0, z)$, $\Gamma_2(x_0, z)$ are given by Eqs (33) and (34) with $x = x_0$. Eq. (43) can be approximated by

$$\dot{i}_h \approx \kappa_0 \frac{z_1 - z_0}{2} \sum_{i=1}^N w_i q \left(\frac{\xi_i (z_1 - z_0) + z_0 + z_1}{2} \right) \quad (45)$$

where ξ_i and w_i are given in Table I.

Example 6 Consider a square vertical blast deflector of area $\mathbb{A} = 1 \text{ m}^2$ and centered on the x axis. Let us predict the total impulse when $x_0 \in [0, \infty)$ and the remaining mine and plate geometries are as those of Ex. 1 on page 9. Eq. (44), with the use of Eqs (39) and (40) for a symmetric problem, is plotted in Fig. 15. This function was then integrated with a 4-point quadrature (Eq. (45)) and plotted in dashed lines in Fig. 16; the solid line is the solution of Eq. (42) directly from *Mathematica*TM. Discrepancies between the two curves arise from the difference between $f(\zeta d)$ and $g(\zeta d)$ for $\zeta d > 2.5$ (Fig. 3).

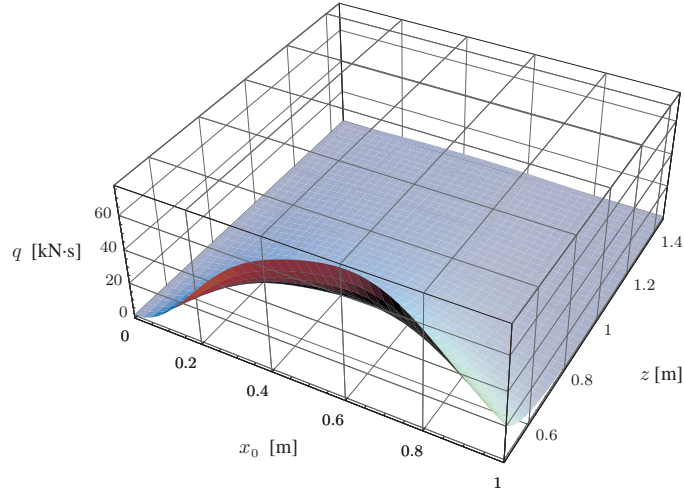


FIGURE 15 – Graph of Eq. (44) for Ex. 6

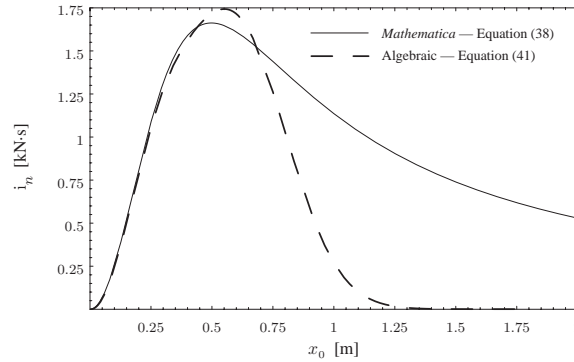


FIGURE 16 – Total Impulse as a Function of x_0 for Ex. 6

Ex. 6 above illustrates how the specific impulse modeled by Westin et al. in [4] is sensitive to the lateral distance $d = \sqrt{x^2 + y^2}$ from the center of the mine. In Ex. 3 on page 11, the effect of the impulse is still being felt 4 m above the mine (Fig. 7). However, in Ex. 6, the maximum impulse is at a lateral distance of 50 cm, and drops rapidly after that (Fig. 16). In both cases, the plate was 1 m^2 . That is a consequence

of the assumptions that the loading produced from a landmine explosion is mainly the result of detonation products and soil ejecta, which are propelled upwards like in a cone, and that blast overpressure plays only a secondary role.

Example 7 Consider the V-shaped deflector in Fig. 17 where γ varies from 0 (a vertical plate) to 180 deg (a horizontal plate). The two 1 m long plates are centered above the mine and the total deflector has a presented area $\mathbb{A} = 1 \text{ m}^2$ on the \mathbf{xy} plane for $\gamma > 0$. The total impulse on the deflector is twice the impulse on one single plate. Then,

$$\begin{aligned} \gamma &\in [0, 180] \quad [\text{deg}] \\ \alpha &= \pi \left(1 - \frac{\gamma}{360} \right) \quad [\text{rad}] \\ x_0 &= 0 \\ x_1 &= 0.5 \quad [\text{m}] \\ z_0 &= \lambda = 0.47 \quad [\text{m}] \\ z_1 &= \lambda - 0.5 \cot \alpha \quad [\text{m}] \\ y &\in [-0.5, 0.5] \quad [\text{m}] \end{aligned}$$

and the impulse is twice the value predicted by Eqs (11), (38) or (45). The total impulse for selected angles γ are given in Table II and plotted at Fig. 18 along with Eq. (38), using $N = 4$.

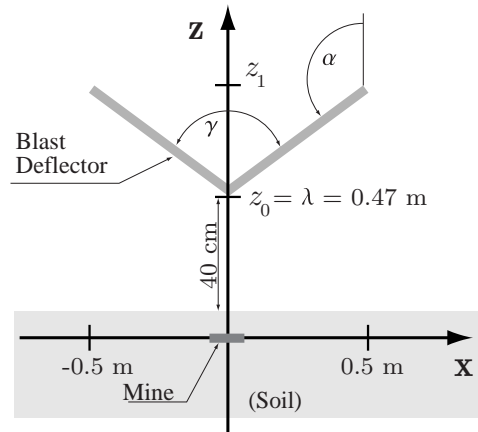


FIGURE 17 – V-Shaped deflector of Variable Angle γ

TABLE II
Impulse on the Variable V-Shaped Deflector for Ex. 7

γ [deg]	α [rad]	Equation used	Impulse [kN·s]
0	π	(45)	0
22.5	$15\pi/16$	(38)	0.5
45	$7\pi/8$	(38)	1.7
90	$3\pi/4$	(38)	5.5
135	$5\pi/8$	(38)	10.6
180	$\pi/2$	(11)	17.4

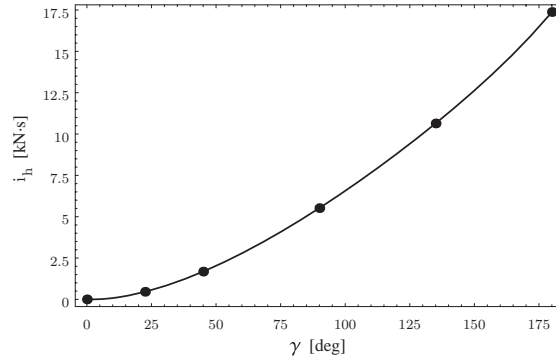


FIGURE 18 – Impulse as a Function of the Angle γ in Fig. 17

7 CONCLUSIONS

Algebraic equations were derived to predict the total impulse on a flat blast deflector at an arbitrary orientation. Furthermore, a very simple equation predicting the maximum impulse at a given standoff distance was also derived. These equations can easily be coded in either a spreadsheet or a computer program.

As they stand, these equations are an aid to engineers who need to estimate the loadings to be expected for the design of blast deflectors. However, more research is required to model and predict the effects of the impulse produced from a mine explosion under a wheel combined with blast deflectors loadings.

8 ACKNOWLEDGMENTS

I am indebted to Dr. Claude Fortier for having raised the cosine squared relation in Chapter 5 and for his meticulous cross-checking of the results presented throughout the examples.

9 REFERENCES

1. Army Lessons Learned Center. Poster on Mine Incidents. Fort Frontenac, Kingston, Ontario, K7K 5L0.
2. Chief Research & Development. Outline of Program. Research and Development Branch, National Defence Headquarters, June 1996.
3. Chief Research & Development. An Inventory of R&D Activities and Technical Expertise. Research and Development Branch, National Defence Headquarters, September 1997.
4. P.S. Westin, B.L. Morris, P.A. Cox, and E.Z. Polch. Development of Computer Program for Floor Plate Response from Land Mine Explosions. Technical Report No. 13045, US Army Tank-Automotive Command, Warren, MI, January 1985. UNCLASSIFIED.
5. E. Martin, editor. *Mathematica 3.0 — Standard Add-on Packages*. Cambridge University Press, 1996.
6. S. Wolfram. *The Mathematica Book*. Cambridge University Press, 3rd edition, 1996.
7. B.L. Morris. Analysis of Improved Crew Survivability in Light Vehicles Subjected to Mine Blast — Volumes 1 & 2. Technical Report SwRI Project No. 06-5095, US Army Belvoir Research, Development and Engineering Center, Fort Belvoir, Virginia, December 1993. UNCLASSIFIED.
8. B. Carnahan, H.A. Luther, and J.O. Wilkes. *Applied Numerical Methods*. John Wiley & Sons, 1969.
9. W.H. Press, B.P. Flannery, S.A. Teukolsky, and W.T. Vetterling. *Numerical Recipes in C*. Cambridge University Press, 1988.

APPENDIX

The Error Function

The function $\operatorname{erf}(x)$ is the error function defined by

$$\operatorname{erf}(x) = \frac{2}{\sqrt{\pi}} \int_0^x e^{-t^2} dt \equiv \begin{cases} P(\frac{1}{2}, x^2) & \text{if } x \geq 0 \\ -P(\frac{1}{2}, x^2) & \text{if } x < 0 \end{cases}$$

where $P(\frac{1}{2}, x^2)$ is the incomplete gamma function. Reference [9] proposes a Chebyshev fitting for $\operatorname{erf}(x)$ with a fractional error everywhere less than $1.2 \cdot 10^{-7}$:

$$\operatorname{erf}(x) \simeq \begin{cases} 1 - \theta & x \geq 0 \\ \theta - 1 & x < 0 \end{cases}$$

with

$$\begin{aligned} \theta = t \exp(-x^2 - 1.26551223 + t(1.00002368 + t(0.37409196 + \\ t(0.09678418 + t(-0.18628806 + t(0.27886807 + t(-1.13520398 + \\ t(1.48851587 + t(-0.82215223 + 0.17087277t)))))))))) \end{aligned}$$

and

$$t = \frac{1}{1 + \frac{|x|}{2}}.$$